AIAA JOURNAL
Vol. 37, No. 5, May 1999

Buckling and Vibration Analysis of Composite Sandwich Plates with Elastic Rotational Edge Restraints

Masoud Rais-Rohani* and Pierre Marcellier†
Mississippi State University, Mississippi State, Mississippi 39762

The small-deflection theory developed for simply supported orthotropic sandwich plates is extended for the elastic buckling and free vibration analysis of anisotropic rectangular sandwich plates with edges elastically restrained against rotation. The plate deflection and transverse shear forces are represented by an independent set of functions that satisfy the essential boundary conditions for all and the natural boundary conditions for specific cases. The Rayleigh–Ritz method is used to solve for in-plane buckling loads and transverse natural frequencies through the solution of an eigenvalue problem. The numerical tables included demonstrate the effects of elastic edge conditions, aspect ratio, and face sheet ply pattern on the buckling loads and natural frequencies of anisotropic sandwich plates.

Nomenclature

A_{ij}, B_{ij}, D_{ij}	= extension, coupling, and bending stiffness matrices
a, b	= plate dimensions in x and y directions, respectively
E_1, E_2	= elastic moduli in principal material directions
G_{xz}, G_{yz}	= transverse shear moduli of core in x–z and y–z planes, respectively
G_{12}	= in-plane shear modulus in 1–2 plane
h	= total plate thickness
h_c	= core thickness
I_t	= rotary inertia
i, j, m, n	= half-wavelength integers
$\boldsymbol{K}$	= nondimensional rotational stiffness
K_1, K_2, K_3, K_4	= rotational stiffnesses along the edges of the rectangular plate
M, N	= number of terms in the series for w, Q_x, and Q_y
$\boldsymbol{M}$	= vector containing M_x, M_y, M_{xy}
M_x, M_y, M_{xy}	= internal moments per unit length
$\bar{M}_x$, $\bar{M}_y$, $\bar{M}_{xy}$	= external edge moments per unit length
$\boldsymbol{N}$	= vector containing N_x, N_y, N_{xy}
N_{cr}	= buckling load
N_p	= total number of layers in upper and lower face sheets
N_x, N_y, N_{xy}	= internal in-plane direct and shear forces per unit length
$\bar{N}_x$, $\bar{N}_y$, $\bar{N}_{xy}$	= external in-plane direct and shear forces per unit length
$\bar{Q}^k_{ij}$	= transformed reduced stiffness matrix of kth face sheet layer in the plate
Q_x, Q_y	= transverse shear forces in the core in x–z and y–z planes, respectively
S_x, S_y	= transverse shear stiffnesses of the core in x–z and y–z planes, respectively
T	= kinetic energy of the plate
t	= face sheet thickness
u, v, w	= midplane displacements in the x, y, and z directions, respectively
V_b	= strain energy due to bending and twisting of the face sheets
V_e	= potential energy of elastic edge support reactions
V_f	= potential energy due to external in-plane forces
V_s	= strain energy due to shearing of the core
X_m, Y_n, X^x_m, Y^x_n, X^y_m, Y^y_n	= characteristic functions for w, Q_x, and Q_y, respectively
z_k	= z distance to the bottom surface of kth layer
$\boldsymbol{\Gamma}$	= $[\Gamma_{11}, \ldots, \Gamma_{MN}]^T$
Γ_{mn}, Ω_{mn}, Ψ_{mn}	= undetermined coefficients
γ_{xz}, γ_{yz}	= transverse shear strains in the core in x–z and y–z planes, respectively
$\boldsymbol{\varepsilon}$	= vector of in-plane strains $(\varepsilon_x, \varepsilon_y, \gamma_{xy})$ at the middle surface of the plate
θ	= ply orientation angle in a face sheet measured from x axis
$\boldsymbol{\kappa}$	= vector of curvatures $(\kappa_x, \kappa_y, \kappa_{xy})$ at the middle surface of the plate
ν_{12}	= Poisson's ratio
ρ, ρ_c, ρ_k, ρ_t	= material density, core density, density of kth layer, and total plate density, respectively
$\boldsymbol{\Psi}$	= $[\Psi_{11}, \ldots, \Psi_{MN}]^T$
$\boldsymbol{\Omega}$	= $[\Omega_{11}, \ldots, \Omega_{MN}]^T$
ω	= natural frequency

Subscripts

$,t$	= $\partial/\partial t$
$,x$	= $\partial/\partial x$
$,xx$	= $\partial^2/\partial x^2$
$,xy$	= $\partial^2/\partial x \partial y$

Introduction

IN pursuit of reducing the weight of aircraft structures while maintaining the desired level of rigidity, more designers are considering the use of sandwich panels with face sheets made of advanced composite materials. The high rigidity of sandwich panels helps to reduce the number of stiffeners by allowing them to be more widely spaced than otherwise possible. Such a panel could then be treated as a plate with opposite edges supported by two adjacent stringers/longerons and ribs/frames.

In wing structures, upper skin panels are typically designed based on buckling strength, whereas in rotorcraft fuselage structures they are designed based on buckling as well as vibration characteristics. In either case, the assumption of classical boundary conditions, in the form of pinned or clamped edges, might inaccurately estimate the torsional rigidities of the edge supports, resulting in either an inefficient panel design or one with a lower than expected margin of safety. To overcome this problem, we present a method for

Received Feb. 14, 1998; presented as Paper 98-2084 at the AIAA/ASME/ASCE/AHS/ASC 39th Structures, Structural Dynamics, and Materials Conference, Long Beach, CA, April 20–23, 1998; revision received Dec. 23, 1998; accepted for publication Jan. 12, 1999.

*Associate Professor, Department of Aerospace Engineering. Senior Member AIAA.

†Exchange Student, Department of Aerospace Engineering, from French Institute for Advanced Mechanical Engineering, Campus des Cezeaux, BP 265, 63175 Aubiere CEDEX, France.

elastic buckling and free vibration analysis of composite rectangular sandwich plates with edges rigidly supported against transverse displacement but elastically restrained against rotation.

This type of boundary condition appears to have been first considered by Carmichael,[1] who developed an approximate solution for free vibration of isotropic rectangular plates based on the Rayleigh–Ritz method. Laura and Grossi[2] later used the Ritz method with polynomial functions for the free vibration analysis of anisotropic rectangular plates of uniform thickness having all edges elastically restrained against rotation. Warburton and Edney[3] developed a procedure by which the free vibration of isotropic rectangular plates with elastically restrained edges was solved using the vibration modes of similar plates having classical boundary conditions. Recently, Jones and Klang[4] examined the buckling of anisotropic plates with and without cutouts and elastically restrained edges. They also relied on the Rayleigh–Ritz method in their analysis.

Early examples of work on the free vibration of isotropic rectangular sandwich plates with classical boundary conditions are by Yu[5] and Chang et al.[6] Rao and Kaeser[7] and Rao[8] extended the general small-deflection theory of orthotropic sandwich plates developed by Libove and Batdorf[9] to the shear and axial buckling problems of anisotropic sandwich plates with all edges simply supported. Watanabe et al.[10] applied a general finite element method for stiffness and free vibration analysis of anisotropic sandwich plates. Li and Mirza[11] used the reciprocal theorem method and Reissner's theory of finite deflection of sandwich plates for the buckling analysis of clamped sandwich plates. Most recently, Moh and Hwu[12] considered a general scheme for the buckling analysis and design optimization of sandwich plates with anisotropic face sheets and different combinations of classical boundary conditions.

The method presented in this paper provides approximate analytical solutions for the free vibration and buckling of rectangular anisotropic plates as well as rectangular sandwich plates with anisotropic face sheets and orthotropic core. This method has been applied for the solution of several examples with some results compared with those reported in the literature.

Analysis

Theory

The theoretical development is based on the general small-deflection theory for rectangular orthotropic sandwich plates developed by Libove and Batdorf[9] and extended by Rao[8] for buckling analysis of simply supported sandwich plates with anisotropic face sheets. This theory is further extended here for the free vibration and buckling analysis of anisotropic sandwich plates with edges elastically restrained against rotation. In this theory, the plate's curvatures are expressed in terms of lateral deflection of the plate and transverse shear strains in the core. The bending stiffness is assumed to be primarily provided by the face sheets, whereas the transverse shear stiffness is mainly provided by the core. Although the core is assumed to have infinite transverse normal rigidity, its in-plane rigidities are assumed to be insignificant compared to those of the face sheets.

Plate Model

The sandwich plate is composed of thin face sheets of constant thickness separated by and perfectly bonded to an orthotropic core. Each face sheet is made of multiple generally orthotropic layers. The plate is only assumed to be symmetric about its middle surface. The plate geometry and boundary conditions are shown in Fig. 1. The torsional stiffness provided by each edge support is modeled by a series of torsional springs with a combined spring constant of K. For generalization, each edge support is shown to have a different torsional stiffness.

Constitutive and Kinematic Relations

The constitutive relations for the sandwich plate are expressed in matrix form as

$$\begin{Bmatrix} N \\ M \end{Bmatrix} = \begin{bmatrix} A & B \\ B & D \end{bmatrix} \begin{Bmatrix} \varepsilon \\ \kappa \end{Bmatrix} \tag{1}$$

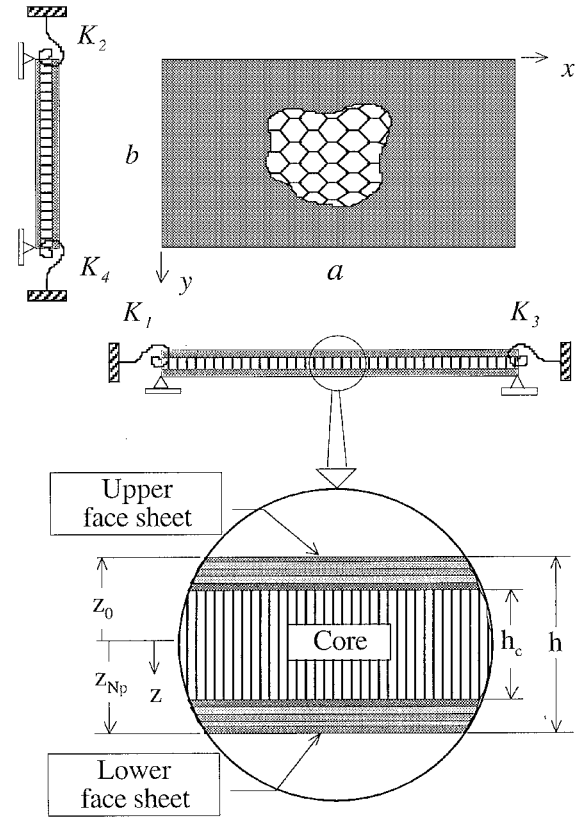

Fig. 1 General description of the sandwich plate model.

$$\begin{Bmatrix} Q_x \\ Q_y \end{Bmatrix} = \begin{bmatrix} S_x & 0 \\ 0 & S_y \end{bmatrix} \begin{Bmatrix} \gamma_{xz} \\ \gamma_{yz} \end{Bmatrix} \tag{2}$$

where A, B, and D are extensional, coupling, and bending rigidities defined as

$$A_{ij} = \sum_{k=1}^{N_p} \bar{Q}_{ij}^k (z_k - z_{k-1}), \qquad B_{ij} = \frac{1}{2} \sum_{k=1}^{N_p} \bar{Q}_{ij}^k (z_k^2 - z_{k-1}^2)$$

$$D_{ij} = \frac{1}{3} \sum_{k=1}^{N_p} \bar{Q}_{ij}^k (z_k^3 - z_{k-1}^3) \tag{3}$$

The coefficient matrix in Eq. (2) consists of tranverse shear rigidities defined as $S_x = h_c G_{xz}$ and $S_y = h_c G_{yz}$. Based on the described theory, only the face sheets contribute to the A, B, and D matrices, whereas only the core contributes to the transverse shear rigidities.

The midplane strains and curvatures are related to the deflections and transverse shear deformations through the kinematic relations

$$\begin{Bmatrix} \varepsilon_x \\ \varepsilon_y \\ \gamma_{xy} \end{Bmatrix} = \begin{Bmatrix} u_{,x} + w_{,x}^2/2 \\ v_{,y} + w_{,y}^2/2 \\ u_{,y} + v_{,x} + w_{,x} w_{,y} \end{Bmatrix} \tag{4a}$$

$$\begin{Bmatrix} k_x \\ k_y \\ k_{xy} \end{Bmatrix} = \begin{Bmatrix} w_{,xx} - Q_{x,x}/S_x \\ w_{,yy} - Q_{y,y}/S_y \\ 2w_{,xy} - Q_{x,y}/S_x - Q_{y,x}/S_y \end{Bmatrix} \tag{4b}$$

Although the in-plane deflections (u and v) can vary through the thickness, the transverse deflection w is assumed to remain constant.

Application of the Rayleigh–Ritz Method

The free vibration and buckling problems are set up and solved using the Rayleigh–Ritz method. For each problem the energy

condition Π is expressed as a function of lateral deflection and transverse shear forces in the core such that for free vibration

$$\Pi(w, Q_x, Q_y) = V_b + V_s + V_e - T \tag{5}$$

and for buckling

$$\Pi(w, Q_x, Q_y) = V_b + V_s + V_e + V_f \tag{6}$$

The strain energy stored in the face sheets and the core can be expressed as

$$\begin{aligned} V_b = \frac{1}{2}\int_0^a\int_0^b \Bigg[& D_{11}\left(w_{,xx} - \frac{Q_{x,x}}{S_x}\right)^2 + 2D_{12}\left(w_{,xx} - \frac{Q_{x,x}}{S_x}\right) \\ & \times \left(w_{,yy} - \frac{Q_{y,y}}{S_y}\right) + D_{22}\left(w_{,yy} - \frac{Q_{y,y}}{S_y}\right)^2 \\ & + 2D_{16}\left(w_{,xx} - \frac{Q_{x,x}}{S_x}\right)\left(2w_{,xy} - \frac{Q_{x,y}}{S_x} - \frac{Q_{y,x}}{S_y}\right) \\ & + 2D_{26}\left(w_{,yy} - \frac{Q_{y,y}}{S_y}\right)\left(2w_{,xy} - \frac{Q_{x,y}}{S_x} - \frac{Q_{y,x}}{S_y}\right) \\ & + D_{66}\left(2w_{,xy} - \frac{Q_{x,y}}{S_x} - \frac{Q_{y,x}}{S_y}\right)^2 \Bigg] \mathrm{d}y\,\mathrm{d}x \end{aligned} \tag{7}$$

$$V_s = \frac{1}{2}\int_0^a\int_0^b \left(\frac{Q_x^2}{S_x} + \frac{Q_y^2}{S_y}\right)\mathrm{d}y\,\mathrm{d}x \tag{8}$$

The potential energy associated with the external in-plane edge forces and elastic edge moments can be expressed as

$$V_f = \frac{1}{2}\int_0^a\int_0^b \left(\bar{N}_x w_{,x}^2 + \bar{N}_y w_{,y}^2 + 2\bar{N}_{xy} w_{,x} w_{,y}\right)\mathrm{d}y\,\mathrm{d}x \tag{9}$$

$$\begin{aligned} V_e = \frac{1}{2}\Bigg\{ & \int_0^a \left[\bar{M}_y\left(w_{,y} - \frac{Q_y}{S_y}\right)\right]_0^b \mathrm{d}x \\ & + \int_0^b \left[\bar{M}_x\left(w_{,x} - \frac{Q_x}{S_x}\right)\right]_0^a \mathrm{d}y \Bigg\} \end{aligned} \tag{10}$$

where $(w_{,x} - Q_x/S_x)$ and $(w_{,y} - Q_y/S_y)$ are the rotations parallel to the x–z and y–z planes, respectively, of an originally vertical line at the edge of the plate. The general expression for the kinetic energy of the plate can be written as[13]

$$T = \frac{1}{2}\int_{-\frac{h}{2}}^{\frac{h}{2}}\int_0^b\int_0^a \rho\left[u_{,t}^2 + v_{,t}^2 + w_{,t}^2\right]\mathrm{d}x\,\mathrm{d}y\,\mathrm{d}z \tag{11}$$

where ρ is the material density, which can vary through the thickness. The integration in Eq. (11) is performed over the plate volume including the core. Assuming in-plane displacements vary linearly through the thickness and that the three displacements are in the form $u = ue^{i\omega t}$, $v = ve^{i\omega t}$, and $w = we^{i\omega t}$, Eq. (11) can be rewritten as

$$T = \frac{1}{2}\omega^2\int_0^a\int_0^b \left[I_t\left(w_{,x}^2 + w_{,y}^2\right) + \rho_t w^2\right]\mathrm{d}y\,\mathrm{d}x \tag{12}$$

where

$$\rho_t = \sum_{k=1}^{N_p+1} \rho_k(z_k - z_{k-1}) \tag{13a}$$

$$I_t = \frac{1}{3}\sum_{k=1}^{N_p+1} \rho_k\left(z_k^3 - z_{k-1}^3\right) \tag{13b}$$

The term involving I_t in Eq. (12) represents the rotary inertia, which, if we assume the slopes $w_{,x}$ and $w_{,y}$ are small, negligibly contributes to the kinetic energy compared to the other term and, hence, can be ignored. Equations (13a) and (13b) include the contribution of the core as well as the face sheets.

The boundary conditions specified earlier are formulated as

$$\begin{aligned} & w = 0, \quad Q_y = 0, \quad \bar{M}_x = -K_1(w_{,x} - Q_x/S_x) \quad \text{at} \quad x = 0 \\ & w = 0, \quad Q_y = 0, \quad \bar{M}_x = K_3(w_{,x} - Q_x/S_x) \quad \text{at} \quad x = a \\ & w = 0, \quad Q_x = 0, \quad \bar{M}_y = -K_2(w_{,y} - Q_y/S_y) \quad \text{at} \quad y = 0 \\ & w = 0, \quad Q_x = 0, \quad \bar{M}_y = K_4(w_{,y} - Q_y/S_y) \quad \text{at} \quad y = b \end{aligned} \tag{14}$$

If, for example, the $x = 0, a$ edges are simply supported, i.e., $K_1 = K_3 = 0$, then the corresponding natural boundary condition becomes $\bar{M}_x = 0$, whereas, if they are clamped, i.e., $K_1 = K_3 = \infty$, then $w_{,x} - Q_x/S_x = 0$.

To proceed with the solutions to the free vibration and elastic buckling problems, suitable functions have to be selected for the transverse deflection and the transverse shear forces such that the boundary conditions given by Eq. (14) are satisfied. In the application of the Rayleigh–Ritz method only the essential boundary conditions are required to be satisfied by the assumed functions for w, Q_x, and Q_y; however, the accuracy and convergence of the solution could be improved if the natural boundary conditions are also satisfied.

The solutions for the free vibration and elastic buckling problems are sought in the form

$$w = \sum_{m=1}^{M}\sum_{n=1}^{N} \Gamma_{mn} X_m(x) Y_n(y) \tag{15}$$

$$Q_x = \sum_{m=1}^{M}\sum_{n=1}^{N} \Omega_{mn} X_m^x(x) Y_n^x(y) \tag{16}$$

$$Q_y = \sum_{m=1}^{M}\sum_{n=1}^{N} \Psi_{mn} X_m^y(x) Y_n^y(y) \tag{17}$$

The X_m and Y_n functions for Q_x and Q_y are distinguished by the use of x and y superscripts, respectively. The finite series are terminated at values of M and N that render sufficiently accurate solution to each problem.

To satisfy the essential boundary conditions and the edge conditions on Q_x and Q_y, we must have

$$X_m = 0 \quad \text{and} \quad X_m^y = 0 \quad \text{at} \quad x = 0, a \tag{18a}$$

$$Y_n = 0 \quad \text{and} \quad Y_n^x = 0 \quad \text{at} \quad y = 0, b \tag{18b}$$

Using Eqs. (1) and (4b) to describe the edge moments, the natural boundary conditions along the $x = 0, a$ edges can be written as

$$\begin{aligned} & -D_{11}\left(w_{,xx} - \frac{Q_{x,x}}{S_x}\right) - D_{12}\left(w_{,yy} - \frac{Q_{y,y}}{S_y}\right) \\ & - D_{16}\left(2w_{,xy} - \frac{Q_{x,y}}{S_x} - \frac{Q_{y,x}}{S_y}\right) = -K_1\left(w_{,x} - \frac{Q_x}{S_x}\right) \end{aligned} \tag{19a}$$

$$\begin{aligned} & -D_{11}\left(w_{,xx} - \frac{Q_{x,x}}{S_x}\right) - D_{12}\left(w_{,yy} - \frac{Q_{y,y}}{S_y}\right) \\ & - D_{16}\left(2w_{,xy} - \frac{Q_{x,y}}{S_x} - \frac{Q_{y,x}}{S_y}\right) = K_3\left(w_{,x} - \frac{Q_x}{S_x}\right) \end{aligned} \tag{19b}$$

Because of the presence of unknown coefficients (Γ_{mn}, Ω_{mn}, and Ψ_{mn}) in the solutions for w, Q_x, and Q_y, Eqs. (19a) and (19b) are broken into three separate parts involving w, Q_x, and Q_y, respectively:

$$D_{11}w_{,xx} + 2D_{16}w_{,xy} = K_1 w_{,x}$$
$$D_{11}w_{,xx} + 2D_{16}w_{,xy} = -K_3 w_{,x} \tag{20a}$$

$$D_{11}Q_{x,x} + D_{16}Q_{x,y} = K_1 Q_x$$
$$D_{11}Q_{x,x} + D_{16}Q_{x,y} = -K_3 Q_x \tag{20b}$$

$$D_{16}Q_{y,x} = 0 \tag{20c}$$

The coefficient of D_{12} term in Eqs. (19a) and (19b) is zero because of the condition specified in Eq. (18a). For sandwich face sheets made of specially orthotropic layers, conditions in Eqs. (20a–20c) are exactly satisfied as D_{16} in such a case would vanish. However, for a more general case involving anisotropic face sheets, D_{16} will not be zero. This complicates the fulfillment of the natural boundary conditions because of the coupling term involving x and y functions. In such a case, the error associated with removing the coupling term from Eqs. (20a–20c) depends on the magnitude of D_{16} compared with that of D_{11}. If the value of D_{16} is negligible compared with that of D_{11}, then the error in this simplication would also be very small. Without the coupling term, the natural boundary conditions along the $x = 0, a$ edges can be expressed as

$$X_{m,xx} = \begin{cases} (K_1/D_{11})X_{m,x} & \text{at} \quad x = 0 \\ -(K_3/D_{11})X_{m,x} & \text{at} \quad x = a \end{cases} \tag{21a}$$

such that

$$X_{m,x}(a) = \begin{cases} -X_{m,x}(0) & (m \text{ odd}) \\ X_{m,x}(0) & (m \text{ even}) \end{cases} \tag{21a$'$}$$

$$X^x_{m,x} = \begin{cases} (K_1/D_{11})X^x_m & \text{at} \quad x = 0 \\ -(K_3/D_{11})X^x_m & \text{at} \quad x = a \end{cases} \tag{21b}$$

such that

$$X^x_m(a) = \begin{cases} X^x_m(0) & (m \text{ odd}) \\ -X^x_m(0) & (m \text{ even}) \end{cases} \tag{21b$'$}$$

The general form of the characteristic beam function

$$F_r(x) = A_r \cosh(\alpha_r x/L) + B_r \sinh(\alpha_r x/L) + C_r \cos(\alpha_r x/L) + D_r \sin(\alpha_r x/L), \qquad r = 1, 2, 3, \ldots \tag{22}$$

is used to describe the X_m function in Eq. (15) with the unknown coefficients A_r, B_r, C_r, D_r, and α determined according to the specified boundary conditions. If, for example, the opposite edges are assumed to have the same rotational stiffness such that $K_1 = K_3 = K$ and $K_2 = K_4 = 0$, then satisfying the specified boundary conditions in Eqs. (18a) and (21a) yields

$$X_m(x) = A_m[\cosh(\alpha_m x/a) - \cos(\alpha_m x/a)] + B_m \sinh(\alpha_m x/a) + \sin(\alpha_m x/a), \qquad m = 1, 2, 3, \ldots, M \tag{23}$$

where, for m odd,

$$A_m = -\cot(\alpha_m/2), \qquad B_m = \cot(\alpha_m/2)\tanh(\alpha_m/2)$$
$$\alpha_m = -\tfrac{1}{2}(aK/D_{11})[\tan(\alpha_m/2) + \tanh(\alpha_m/2)] \tag{24a}$$

and, for m even,

$$A_m = \tan(\alpha_m/2), \qquad B_m = -\tan(\alpha_m/2)\coth(\alpha_m/2)$$
$$\alpha_m = \tfrac{1}{2}(aK/D_{11})[\cot(\alpha_m/2) - \coth(\alpha_m/2)] \tag{24b}$$

For the X_m functions describing the transverse shear forces Q_x and Q_y, the simplified form of Eq. (22) with the hyperbolic terms eliminated is used. This form does satisfy the boundary conditions in Eqs. (18a), (18b), and (21b) and for the case $K_1 = K_3 = K$, and $K_2 = K_4 = 0$ yields

$$X^x_m(x) = C^x_m \cos(\alpha^x_m x/a) + D^x_m \sin(\alpha^x_m x/a) \qquad m = 1, 2, 3, \ldots, M \tag{25}$$

where

$$C^x_m = \frac{\alpha^x_m}{\Delta}, \qquad D^x_m = \frac{aK/D_{11}}{\Delta}, \qquad \Delta = \sqrt{(\alpha^x_m)^2 + \left(\frac{aK}{D_{11}}\right)^2} \tag{26a}$$

$$\alpha^x_m(1 \mp \cos\alpha^x_m) \mp (aK/D_{11})\sin\alpha^x_m = 0 \qquad (m \text{ odd/even}) \tag{26b}$$

$$X^y_m(x) = \sin(\alpha^y_m x/a) \tag{27}$$

$$\alpha^y_m = m\pi, \qquad m = 1, 2, 3, \ldots, M \tag{28}$$

Considering the natural boundary conditions along the $y = 0, b$ edges, the characteristic functions Y_n, Y^x_n, and Y^x_n are found by following similar steps to those shown in Eqs. (19–22).

With the unknown coefficients in the characteristic functions determined, Eqs. (15–17) are substituted into Eqs. (5) and (6) via Eqs. (7–10) and (12). For the Rayleigh–Ritz solutions to the free vibration and elastic buckling problems, Π is minimized with respect to the undetermined coefficients Γ_{mn}, Ω_{mn}, and Ψ_{mn}. That is,

$$\frac{\partial Z}{\partial \Gamma_{mn}} = 0, \qquad \frac{\partial \Sigma}{\partial \Omega_{mn}} = 0, \qquad \frac{\partial \Sigma}{\partial \Psi_{mn}} = 0 \tag{29}$$

where $m = 1, 2, \ldots, M$, $n = 1, 2, \ldots, N$, $\Sigma \equiv V_b + V_s + V_e$, and $Z = \Sigma - T$ (free vibration) and $\Sigma + V_f$ (buckling). These equations lead to a system of 3 $(M \times N)$ linear equations, which in symbolic matrix form may be expressed as

$$\begin{bmatrix} \left[\frac{\partial Z}{\partial \Gamma_{mn}}\Big|_{\Gamma_{ij}}\right] & \left[\frac{\partial \Sigma}{\partial \Gamma_{mn}}\Big|_{\Omega_{ij}}\right] & \left[\frac{\partial \Sigma}{\partial \Gamma_{mn}}\Big|_{\Psi_{ij}}\right] \\ \left[\frac{\partial \Sigma}{\partial \Omega_{mn}}\Big|_{\Gamma_{ij}}\right] & \left[\frac{\partial \Sigma}{\partial \Omega_{mn}}\Big|_{\Omega_{ij}}\right] & \left[\frac{\partial \Sigma}{\partial \Omega_{mn}}\Big|_{\Psi_{ij}}\right] \\ \left[\frac{\partial \Sigma}{\partial \Psi_{mn}}\Big|_{\Gamma_{ij}}\right] & \left[\frac{\partial \Sigma}{\partial \Psi_{mn}}\Big|_{\Omega_{ij}}\right] & \left[\frac{\partial \Sigma}{\partial \Psi_{mn}}\Big|_{\Psi_{ij}}\right] \end{bmatrix} \begin{Bmatrix} \boldsymbol{\Gamma} \\ \boldsymbol{\Omega} \\ \boldsymbol{\Psi} \end{Bmatrix} = \begin{Bmatrix} \mathbf{0} \\ \mathbf{0} \\ \mathbf{0} \end{Bmatrix} \tag{30}$$

where $\boldsymbol{\Gamma} = [\Gamma_{11}, \ldots, \Gamma_{MN}]^T$, $\boldsymbol{\Omega} = [\Omega_{11}, \ldots, \Omega_{MN}]^T$, and $\boldsymbol{\Psi} = [\Psi_{11}, \ldots, \Psi_{MN}]^T$. The coefficient matrix in Eq. (30) is symmetric with each submatrix defined as

$$\frac{\partial \Sigma}{\partial \Gamma_{mn}}\Big|_{\Gamma_{ij}} = \frac{1}{2}\sum_{i=1}^{M}\sum_{j=1}^{N}\Bigg[2\frac{D_{11}b}{a^3}\left(N^{ww}_{im}M^{ww}_{jn}\right) + 2\frac{D_{12}}{ab}\left(E^{ww}_{mi}F^{ww}_{jn} + E^{ww}_{im}F^{ww}_{nj}\right) + 2\frac{D_{22}a}{b^3}\left(L^{ww}_{im}P^{ww}_{jn}\right) + 8\frac{D_{66}}{ab}\left(H^{ww}_{im}K^{ww}_{jn}\right) + 4\frac{D_{16}}{a^2}\left(I^{ww}_{im}J^{ww}_{nj} + I^{ww}_{mi}J^{ww}_{jn}\right) + 4\frac{D_{26}}{b^2}\left(G^{ww}_{mi}O^{ww}_{jn} + G^{ww}_{im}O^{ww}_{nj}\right)\Bigg]\Gamma_{ij} \tag{31}$$

$$\frac{\partial T}{\partial \Gamma_{mn}}\Big|_{\Gamma_{ij}} = \omega^2\sum_{i=1}^{M}\sum_{j=1}^{N}\left[ab\rho_t\left(L^{ww}_{im}M^{ww}_{jn}\right) + I_t\left(\frac{b}{a}H^{ww}_{im}M^{ww}_{jn} + \frac{a}{b}L^{ww}_{im}K^{ww}_{jn}\right)\right]\Gamma_{ij} \tag{32}$$

$$\left.\frac{\partial V_f}{\partial \Gamma_{mn}}\right|_{\Gamma_{ij}} = \sum_{i=1}^{M}\sum_{j=1}^{N}\left(N_x\frac{b}{a}H_{im}^{ww}M_{jn}^{ww} + N_y\frac{a}{b}L_{im}^{ww}K_{jn}^{ww} + 2N_{xy}G_{im}^{ww}J_{nj}^{ww}\right)\Gamma_{ij} \tag{33}$$

$$\left.\frac{\partial \Sigma}{\partial \Gamma_{mn}}\right|_{\Omega_{ij}} = \frac{1}{2S_x}\sum_{i=1}^{M}\sum_{j=1}^{N}\left[\frac{D_{11}b}{a^2}\left(-2I_{im}^{xw}M_{jn}^{xw} + H_{im}^{1}M_{jn}^{xw} + E_{im}^{1}M_{jn}^{xw}\right) - 2\frac{D_{12}}{b}\left(G_{mi}^{wx}F_{jn}^{xw}\right) - 4\frac{D_{66}}{b}\left(G_{im}^{xw}K_{nj}^{wx}\right) + \frac{D_{16}}{a}\left(-4H_{mi}^{wx}J_{jn}^{xw} - 2E_{im}^{xw}J_{nj}^{wx} + G_{im}^{1}J_{nj}^{wx} + 2G_{im}^{1}J_{jn}^{xw}\right) + \frac{D_{26}a}{b^2}\left(-2L_{im}^{xw}O_{jn}^{xw} + L_{im}^{xw}K_{jn}^{2}\right)\right]\Omega_{ij} \tag{34}$$

$$\left.\frac{\partial \Sigma}{\partial \Gamma_{mn}}\right|_{\Psi_{ij}} = \frac{1}{2S_y}\sum_{i=1}^{M}\sum_{j=1}^{N}\left\{\frac{D_{22}a}{b^2}L_{im}^{yw}\left(-2O_{jn}^{yw} + K_{jn}^{1} + F_{jn}^{1}\right) - 2\frac{D_{12}}{a}\left(E_{im}^{yw}J_{nj}^{wy}\right) - 4\frac{D_{66}}{a}\left(H_{im}^{yw}J_{jn}^{yw}\right) + \frac{D_{16}b}{a^2}\left(-2I_{im}^{yw} + H_{im}^{2}\right)M_{jn}^{yw} + \frac{D_{26}}{b}\left[G_{im}^{yw}\left(-4K_{jn}^{yw} + 2J_{jn}^{1}\right) + G_{mi}^{wy}\left(-2K_{jn}^{yw} + J_{jn}^{1}\right)\right]\right\}\Psi_{ij} \tag{35}$$

$$\left.\frac{\partial \Sigma}{\partial \Omega_{mn}}\right|_{\Omega_{ij}} = \frac{1}{2}\sum_{i=1}^{M}\sum_{j=1}^{N}\left\{\frac{D_{11}}{S_x^2}\frac{b}{a}\left[M_{jn}^{xx}\left(2H_{im}^{xx} - G_{mi}^{2} - G_{im}^{2}\right)\right] + 2\frac{D_{66}}{S_x^2}\frac{a}{b}L_{im}^{xx}K_{jn}^{xx} + 2\frac{ab}{S_x}L_{im}^{xx}M_{jn}^{xx} + \frac{D_{16}}{S_x^2}\left(2G_{mi}^{xx}J_{jn}^{xx} + 2G_{im}^{xx}J_{nj}^{xx} - L_{im}^{1}M_{jn}^{2}\right)\right\}\Omega_{ij} \tag{36}$$

$$\left.\frac{\partial \Sigma}{\partial \Psi_{mn}}\right|_{\Psi_{ij}} = \frac{1}{2}\sum_{i=1}^{M}\sum_{j=1}^{N}\left\{\frac{D_{22}}{S_y^2}\frac{a}{b}\left[2L_{im}^{yy}K_{jn}^{yy} - L_{mi}^{yy}\left(J_{nj}^{2} + J_{jn}^{2}\right)\right] + 2\frac{D_{66}}{S_y^2}\frac{b}{a}H_{im}^{yy}M_{jn}^{yy} + 2\frac{ab}{S_y}L_{im}^{yy}M_{jn}^{yy} + \frac{D_{26}}{S_y^2}\left(2G_{im}^{yy}J_{nj}^{yy} + 2G_{mi}^{yy}J_{jn}^{yy} - M_{nj}^{1}L_{im}^{2}\right)\right\}\Psi_{ij} \tag{37}$$

$$\left.\frac{\partial \Sigma}{\partial \Omega_{mn}}\right|_{\Psi_{ij}} = \frac{1}{S_xS_y}\sum_{i=1}^{M}\sum_{j=1}^{N}\left[D_{12}G_{im}^{yx}J_{nj}^{xy} + D_{66}G_{mi}^{xy}J_{jn}^{yx} + D_{16}\frac{b}{a}\left(H_{mi}^{xy} - \frac{1}{2}G_{mi}^{3}\right)M_{nj}^{xy} + D_{26}\frac{a}{b}\left(K_{jn}^{yx} - \frac{1}{2}J_{jn}^{3}\right)L_{im}^{yx}\right]\Psi_{ij} \tag{38}$$

The terms with alphabetical and numerical superscripts in Eqs. (31–38) are defined in the Appendix. Through Gaussian elimination, Eq. (30) is reduced to a simplified eigenvalue problem in the form

$$[[R_1] - \lambda[I]]\{\mathbf{\Gamma}\} = \{\mathbf{0}\} \tag{39}$$

with

$$\{\mathbf{\Omega}\} = (1/\lambda)[R_2]\{\mathbf{\Gamma}\}, \qquad \{\mathbf{\Psi}\} = (1/\lambda)[R_3]\{\mathbf{\Gamma}\} \tag{40}$$

The solution of Eq. (39) results in $M \times N$ eigenvalues, where, for a specified plate aspect ratio, the largest positive eigenvalue gives the natural frequency as $\omega = \sqrt{(1/\lambda_{cr})}$ and the buckling load as $N_{cr} = 1/\lambda_{cr}$. The coefficient matrices R_1, R_2, and R_3 depend on the geometric attributes and material properties of the sandwich plate. Whereas the R_1 matrix for the free vibration problem is different from that for the buckling, R_2 and R_3 matrices remain the same for both problems.

Numerical Results and Discussion

A computer code, based on the described analysis procedure, was developed and used for the analysis of a number of test cases. The results are presented in two parts. The first part is for free vibration (with the rotary inertia term ignored), and the second is for elastic buckling.

It is important to point out that the accuracy of solutions based on the approach presented depends on the values selected for M and N. For low aspect ratio ($a/b < 3$) simply supported sandwich plates with orthotropic face sheets, sufficiently accurate results can be obtained for compression and shear buckling loads, as well as fundamental natural frequency, using M and $N < 4$, but in the presence of anisotropic face sheets and elastic rotational edge restraints, higher values may become necessary. However, higher values for M and N would result in a greater number of algebraic equations whose solutions would be obtained at a greater computational cost. In all of the solutions presented, M and N were set equal to 4.

Results of Vibration Analysis

The results of free vibration analysis obtained are given in Tables 1–5. In the case of isotropic and orthotropic rectangular plates our results for natural frequencies and mode shapes coincide with those previously reported in the literature.[1,14] We also find our results for the case of isotropic sandwich plates with all edges clamped to be in reasonably good agreement with the experimental values reported by Ueng.[15] This agreement resulted although for our calculations we ignored the effects of rotary inertia and truncated the series in Eqs. (15–17) at $M = N = 4$.

We also compared our results for sandwich plates with orthotropic and anisotropic face sheets and all edges clamped with those found numerically by Watanabe et al.[10] using the finite element method. We find that on average our predicted values for natural frequencies are 5% larger than theirs. This is possibly in part because they assume shear strains in the core γ_{xz} and γ_{yz} to be linear functions of the slopes $w_{,x}$ and $w_{,y}$, respectively, whereas in our study these strains are modeled independently of the transverse deflection according to Eqs. (16) and (17). Also by truncating the series in Eqs. (15–17) at $M = N = 4$, our plate model has become somewhat stiffer than theirs, thus resulting in slightly larger values for predicted natural frequencies.

Table 1 Nondimensionalized frequencies $\omega b^2\sqrt{(\rho h/D)}$ of isotropic rectangular plates ($K_1 = K_3 = aK/D = K_2 = K_4 = bK/D = K$)

		Mode number					
		1		2		3	
a/b	K	Present study	Carmichael[1]	Present study	Carmichael[1]	Present study	Carmichael[1]
1	0	19.74	19.74	49.35	49.35	78.96	78.96
	20	31.09	31.09	64.34	64.31	95.89	95.85
	∞	36.01	35.99	73.46	73.41	108.37	108.3
5	0	10.26	10.26	11.45	11.45	13.42	13.42
	20	19.38	19.38	20.15	20.15	21.54	21.52
	∞	22.64	22.64	23.46	23.45	24.93	24.89

Table 2 Nondimensionalized fundamental frequencies $\omega a^2\sqrt{(\rho/h^2E_2)}$ of symmetric cross-ply (0/90/0) square plates[a] ($K_1 = K_3 = aK/D_{11}$ and $K_2 = K_4 = bK/D_{22}$)

		E_1/E_2					
		10		20		30	
aK/D_{11}	bK/D_{22}	Present study	Reddy[14]	Present study	Reddy[14]	Present study	Reddy[14]
0	0	10.65	10.650	13.95	13.948	16.61	16.605
0.25	0.25	11.06	——	14.54	——	17.34	——
20	20	19.14	——	25.91	——	31.24	——
∞	0	21.12	21.118	29.17	29.166	35.43	35.431
∞	∞	22.31	——	30.28	——	36.50	——

[a]$G_{12}/E_2 = 0.6$ and $\nu_{12} = 0.25$.

Table 3 Natural frequencies of aluminum/aluminum honeycomb rectangular sandwich plates[a] ($K_1 = K_3 = aK/D = K_2 = K_4 = bK/D = K$)

		f_{mn}, Hz					
		1		2		3	
K[b]	$m\backslash n$	Present study	Ueng[15]	Present study	Ueng[15]	Present study	Ueng[15]
0	1	27.73	27.759	84.46	84.801	173.18	174.625
	2	51.80	51.880	107.72	108.802	195.27	196.962
	3	91.48	91.704	146.10	146.857	231.75	233.889
∞	1	51.57	48	123.54	127	224.68	238
	2	77.83	84	147.57	148	247.48	249
	3	122.33	137	189.28	192	288.40	285

[a]Properties: $a = 67.75$ in., $b = 43.5$ in., $\rho = 1.114 \times 10^{-5}$ lb-s^2/in.^{3}, $E = 10 \times 10^6$ psi, $\nu = 0.33$, $t = 0.016$ in., $h_c = 0.25$ in., $G_{xz} = 19.5$ ksi, and $G_{yz} = 7.5$ ksi.
[b]$K = 0$ values found by Ueng[15] are theoretical, whereas those for $K = \infty$ are experimental.

Table 4 Natural frequencies of orthotropic and anisotropic $(\theta_1/\theta_2/\theta_3/\text{core})_s$ rectangular sandwich plates[a] ($K_1 = K_3 = K_2 = K_4 = \infty$)

		Mode number f, Hz					
		1		2		3	
$\theta_1/\theta_2/\theta_3$, deg	h_c, mm	Present study	Watanabe et al.[10] (% diff.)	Present study	Watanabe et al.[10] (% diff.)	Present study	Watanabe et al.[10] (% diff.)
30/30/30	10	778	732 (6.28)	1293	1197 (8.02)	1599	1477 (8.26)
0/0/0	10	752	716 (5.03)	1312	1240 (5.81)	1527	1414 (7.99)
30/−30/30	7	642	616 (4.22)	1170	1106 (5.79)	1273	1204 (5.73)
0/90/0	7	716	693 (3.32)	1167	1119 (4.29)	1497	1412 (6.02)

[a]Properties: $a = 450$ mm, $b = 300$ mm, $t = 0.375$ mm, $E_1 = 105$ GPa, $E_2 = 8.74$ GPa, $G_{12} = 4.56$ GPa, $\nu_{12} = 0.327$, $\rho_f = 1600$ kg/m^3, $G_{xz} = 103$ MPa, $G_{yz} = 62.1$ MPa, and $\rho_c = 16$ kg/m^3.

Table 5 Nondimensional fundamental frequencies $\omega b^2\sqrt{(\rho_t/D_{11})}$ of carbon-epoxy/aluminum honeycomb rectangular sandwich plates[a] ($K_1 = K_3 = 0$ and $K_2 = K_4 = bK/D_{22}$)

	bK/D_{22}						
a/b	0	0.5	1	5	10	20	∞
			$[(0/90)_2/\text{core}]_s$, $D_{16}/D_{11} = D_{26}/D_{11} = 0$				
0.5	26.73	26.83	26.91	27.26	27.45	27.67	28.18
1.0	11.89	12.15	12.35	13.18	13.61	14.04	14.97
1.5	9.04	9.39	9.67	10.75	11.28	11.80	12.89
2.5	8.01	8.42	8.74	9.95	10.53	11.09	12.24
			$[0/\pm45/90/\text{core}]_s$, $D_{16}/D_{11} = D_{26}/D_{11} = 0.0066$				
0.5	30.48	30.50	30.51	30.61	30.73	30.92	31.54
1.0	14.76	14.90	15.02	15.55	15.88	16.27	17.25
1.5	11.10	11.36	11.58	12.49	12.97	13.48	14.61
2.5	9.09	9.47	9.78	11.02	11.63	12.22	13.45

[a]Properties: $b = 254$ mm, $t_{\text{ply}} = 0.127$ mm, $E_1 = 229$ GPa, $E_2 = 13.35$ GPa, $G_{12} = 5.25$ GPa, $\nu_{12} = 0.315$, $h_c = 10$ mm, $G_{xz} = 0.146$ GPa, and $G_{yz} = 0.0904$ GPa.

Table 6 Axial buckling of graphite-epoxy/aluminum honeycomb $[(0/90)_2/\text{core}]_s$ rectangular sandwich plates[a] ($K_1 = K_3 = K_2 = K_4 = 0$)

		$N_{x\,\text{cr}}$, N/mm	
a, mm	b, mm	Present study	Moh and Hwu[12]
500	1000	114.19	114.194
1000	1000	60.05	60.0532
2000	1000	60.05	60.0519

[a]Properties: $t_{\text{ply}} = 0.125$ mm, $E_1 = 181$ GPa, $E_2 = 10.3$ GPa, $G_{12} = 7.17$ GPa, $\nu_{12} = 0.28$, $h_c = 10$ mm, $G_{xz} = 0.146$ GPa, and $G_{yz} = 0.0904$ GPa.

To investigate the effect of rotational edge restraints on the vibration characteristics of composite sandwich plates, we analyzed a series of sandwich plates with two opposite edges simply supported and the other two rigidly supported against transverse displacement but elastically restrained against rotation. The results of this analysis are given in Table 5. Because of higher bending stiffness, the sandwich plates with quasi-isotropic face sheets are found to have higher natural frequencies than those of equal thickness cross-ply face sheets.

Regardless of face sheet design, we find that at low aspect ratios the plate rigidity dominates its vibration response with the boundary conditions having a very minor role. However, as the aspect ratio is

increased, the plate becomes more flexible, and the edge conditions become more significant. For example, for the sandwich plate with cross-ply face sheets, the difference between the natural frequency for all edges simply supported vs the one with two opposite edges pinned and the other two clamped is only about 5% for $a/b = 0.5$, but it jumps to 53% for $a/b = 2.5$. This clearly demonstrates the need for proper modeling of torsional stiffness provided by edge stiffeners in a high apect ratio sandwich panel.

Table 7 Axial buckling of carbon-epoxy/aluminum honeycomb $(\theta/\text{core})_s$ square sandwich plates[a] ($K_1 = K_3 = K_2 = K_4 = 0$)

Face sheet	$N_{x\,\text{cr}}$, N/mm		
θ, deg	Present study	Rao[8]	Moh and Hwu[12]
0	423.8	423.8	424.2
10	428.8	428.7	429.3
20	443.5	443.5	444.3
30	459.5	459.5	460.7
40	468.6	468.7	470.1
45	463.3	——	464.9
50	433.7	——	435.2
60	356.5	356.6	357.9
70	285.7	285.6	286.9
80	233.6	233.6	234.8
90	213.8	213.8	214.9

[a]Properties: $a = b = 225$ mm, $t_{\text{ply}} = 0.2$ mm, $E_1 = 229$ GPa, $E_2 = 13.35$ GPa, $G_{12} = 5.25$ GPa, $\nu_{12} = 0.315$, $h_c = 10$ mm, $G_{xz} = 0.146$ GPa, and $G_{yz} = 0.0904$ GPa.

Results of Buckling Analysis

The results of buckling analysis are given in Tables 6–10. The effects of aspect ratio, face sheet ply angle, and boundary condition on buckling load are demonstrated in these solutions. We performed a convergence study on the axial buckling of a simply supported square sandwich plate with each face sheet made of a single ply of an anisotropic material. The values of M and N for w, Q_x, and Q_y functions were kept the same and varied from 1 to 4, and the results were examined for different face sheet ply angles. For angles below 40 deg, there was no improvement in calculated axial buckling loads beyond $M = N = 1$. However, for ply angles above 40 deg, the solutions for buckling loads converged at $M = N = 3$, with minor improvement using $M = N = 4$ (Ref. 16). In Table 7 the critical axial buckling loads obtained here using $M = N = 4$ are compared with those reported by Rao[8] and Moh and Hwu[12] for 11 different ply angles. Our results are found to be in excellent agreement with those reported in the literature for both simply supported and clamped boundary conditions.

We also examined the axial and shear buckling of anisotropic rectangular sandwich plates with two edges simply supported and the other two elastically restrained against rotation. Using conditions similar to those in Table 5, we find, because of higher bending stiffness, the sandwich plates with quasi-isotropic face sheets have higher buckling loads than those with cross-ply face sheets (Tables 9 and 10). In both cases, the sandwich plate is stronger in shear than in axial buckling. We also notice, as in the case of free vibration, the effect of edge condition on buckling becoming more critical as the aspect ratio is increased. However, unlike free vibration, we

Table 8 Axial buckling of graphite-epoxy/aluminum honeycomb $[(\theta/-\theta)_2/\text{core}]_s$ rectangular sandwich plates[a]

		$K_1 = K_3 = K_2 = K_4 = 0$			$K_1 = K_3 = 0; K_2 = K_4 = \infty$		
			$N_{x\,\text{cr}}$, N/mm			$N_{x\,\text{cr}}$, N/mm	
a, mm	b, mm	θ, deg	Present study	Moh and hwu[12]	θ, deg	Present study	Moh and Hwu[12]
1000	500	44	352.68	352.66	36	453.89	444.73
1000	1000	45	99.93	99.932	42	154.78	152.85
1000	2000	0	50.31	50.310	0	51.48	51.488

[a]Properties: $t_{\text{ply}} = 0.125$ mm, $E_1 = 181$ GPa, $E_2 = 10.3$ GPa, $G_{12} = 7.17$ GPa, $\nu_{12} = 0.28$, $h_c = 10$ mm, $G_{xz} = 0.146$ GPa, and $G_{yz} = 0.0904$ GPa.

Table 9 Nondimensional axial buckling loads $N_x b^2/D_{11}$ of carbon-epoxy/aluminum honeycomb rectangular sandwich plates[a] ($K_1 = K_3 = 0$ and $K_2 = K_4 = bK/D_{22}$)

	bK/D_{22}						
a/b	0	0.5	1	5	10	20	∞
			$[(0/90)_2/\text{core}]_s$, $D_{16}/D_{11} = D_{26}/D_{11} = 0$				
0.5	18.10	18.24	18.35	18.82	19.09	19.39	20.11
1.0	14.31	14.95	15.46	17.61	18.76	19.39	20.11
1.5	14.88	15.22	15.49	16.65	17.28	17.95	19.51
2.5	14.43	14.86	15.20	16.65	17.44	18.21	19.30
			$(0/\pm 45/90/\text{core})_s$, $D_{16}/D_{11} = D_{26}/D_{11} = 0.0066$				
0.5	23.54	23.56	23.58	23.74	23.91	24.21	25.19
1.0	22.06	22.49	22.85	23.74	23.91	24.21	25.19
1.5	21.44	21.60	21.73	22.40	22.89	23.56	25.19
2.5	21.41	21.64	21.84	22.55	22.85	23.31	24.73

[a]Same properties as those in Table 5.

Table 10 Nondimensional shear buckling loads $N_{xy} b^2/D_{11}$ of carbon-epoxy/aluminum honeycomb rectangular sandwich plates[a] ($K_1 = K_3 = 0$ and $K_2 = K_4 = bK/D_{22}$)

	bK/D_{22}						
a/b	0	0.5	1	5	10	20	∞
			$[(0/90)_2/\text{core}]_s$, $D_{16}/D_{11} = D_{26}/D_{11} = 0$				
0.5	26.52	31.32	31.20	30.52	30.18	30.18	31.34
1.0	18.46	19.45	19.53	19.72	19.81	20.03	20.80
1.5	16.48	17.12	17.27	17.74	17.99	18.39	19.25
2.5	15.66	15.98	16.19	17.00	17.47	18.05	19.41
			$(0/\pm 45/90/\text{core})_s$, $D_{16}/D_{11} = D_{26}/D_{11} = 0.0066$				
0.5	34.52	40.80	40.62	39.56	38.97	38.74	39.97
1.0	25.22	26.73	26.71	26.53	26.47	26.61	27.47
1.5	22.95	23.75	23.83	24.08	24.26	24.61	25.51
2.5	22.23	22.50	22.64	23.27	23.71	24.31	25.85

[a]Same properties as those in Table 5.

find the effect of boundary condition on both axial and shear buckling to be much greater for sandwich plates with cross-ply face sheets than those with quasi-isotropic facings.

Concluding Remarks

We presented an extension of the small-deflection theory of sandwich plates to the free vibration and buckling analysis of anisotropic sandwich plates with edges rigidly supported against transverse displacement and elastically restrained against rotation. The comparison of results found here with those reported in the literature indicates that natural frequencies, mode shapes, and buckling loads can be predicted with considerable accuracy using the method presented. Although in the example problems the opposite edges of the plate were assumed to have identical conditions, the theory presented is general enough to allow each of the four edges to have a different rotational stiffness. We also found that in both free vibration and buckling of anisotropic sandwich plates, the effect of boundary condition becomes more significant as the aspect ratio is increased.

Appendix: Mathematical Definitions

The terms with alphabetical superscripts in Eqs. (31–38) represent the following integral equations:

$$E_{im}^{ww} = a\int_0^a X_i X_{m,xx}\,\mathrm{d}x, \qquad F_{jn}^{ww} = b\int_0^b Y_j Y_{n,yy}\,\mathrm{d}y$$

$$G_{im}^{ww} = \int_0^a X_i X_{m,x}\,\mathrm{d}x, \qquad H_{im}^{ww} = a\int_0^a X_{i,x} X_{m,x}\,\mathrm{d}x$$

$$I_{im}^{ww} = a^2\int_0^a X_{i,x} X_{m,xx}\,\mathrm{d}x, \qquad J_{jn}^{ww} = \int_0^b Y_j Y_{n,y}\,\mathrm{d}y$$

$$K_{jn}^{ww} = b\int_0^b Y_{j,y} Y_{n,y}\,\mathrm{d}y, \qquad L_{im}^{ww} = \frac{1}{a}\int_0^a X_i X_m\,\mathrm{d}x \tag{A1}$$

$$M_{jn}^{ww} = \frac{1}{b}\int_0^b Y_j Y_n\,\mathrm{d}y, \qquad N_{im}^{ww} = a^3\int_0^a X_{i,x} X_{m,xxx}\,\mathrm{d}x$$

$$\frac{1}{a}\int_0^a X_{i,xx} X_{m,xx}\,\mathrm{d}x = \frac{1}{a^4}N_{im}^{ww} + \frac{1}{a}[X_{i,x} X_{m,xx}]_0^a$$

$$O_{jn}^{ww} = b^2\int_0^b Y_{j,y} Y_{n,yy}\,\mathrm{d}y, \qquad P_{jn}^{ww} = b^3\int_0^b Y_{j,y} Y_{n,yyy}\,\mathrm{d}y$$

$$\frac{1}{b}\int_0^b Y_{j,yy} Y_{n,yy}\,\mathrm{d}y = \frac{1}{b^4}P_{kn}^{ww} + \frac{1}{b}[Y_{j,y} Y_{n,yy}]_0^b$$

For integrals involving different X and Y functions, we use the same notations as Eqs. (A1) with superscripts changed according to the functions involved. For example,

$$L_{im}^{xy} = \frac{1}{a}\int_0^a X_i^x X_m^y\,\mathrm{d}x, \qquad L_{im}^{xw} = \frac{1}{a}\int_0^a X_i^x X_m\,\mathrm{d}x$$

To evaluate each integral in Eqs. (A1) we use a generic formulation based on the characteristic function for a beam of length L given as

$$F_r(x) = A_r\cosh(\alpha_r x/L) + B_r\sinh(\alpha_r x/L) + C_r\cos(\alpha_r x/L) + D_r\sin(\alpha_r x/L) \tag{A2}$$

along with the conditions that, for r odd,

$$F_r(L) = F_r(0), \qquad F_{r,x}(L) = -F_{r,x}(0)$$
$$F_{r,xx}(L) = F_{r,xx}(0), \qquad F_{r,xxx}(L) = -F_{r,xxx}(0) \tag{A3}$$

and, for r even,

$$F_r(L) = -F_r(0), \qquad F_{r,x}(L) = F_{r,x}(0)$$
$$F_{r,xx}(L) = -F_{r,xx}(0), \qquad F_{r,xxx}(L) = F_{r,xxx}(0) \tag{A4}$$

In the case where $\alpha_r \neq \alpha_s$ for r odd, s even or r even, s odd, we have

$$L^2\int_0^L F_{r,x} F_{s,xx}\,\mathrm{d}x = \frac{2}{\alpha_r^4 - \alpha_s^4}\big[\alpha_s^5\alpha_r(B_s + D_s)(B_r + D_r) + \alpha_r^3\alpha_s^3(B_s - D_s)(B_r - D_r) - \alpha_r^2\alpha_s^4(A_s + C_s)(A_r - C_r) - \alpha_s^2\alpha_r^4(A_r + C_r)(A_s - C_s)\big] \tag{A5}$$

$$\int_0^L F_r F_{s,x}\,\mathrm{d}x = \frac{2}{\alpha_r^4 - \alpha_s^4}\big[-\alpha_s^3\alpha_r(B_s - D_s)(B_r + D_r) - \alpha_r^3\alpha_s(B_s + D_s)(B_r - D_r) + \alpha_s^4(A_s + C_s)(A_r + C_r) + \alpha_r^2\alpha_s^2(A_r - C_r)(A_s - C_s)\big] \tag{A6}$$

For the case where $F_r = F_s$ and $\alpha_r = \alpha_s$, the integrals in Eqs. (A5) and (A6) become (due to symmetry)

$$L^2\int_0^L F_{r,x} F_{r,xx}\,\mathrm{d}x = L^2\left[\frac{1}{2}F_{r,x}^2\right]_0^L = 0$$
$$\int_0^L F_r F_{r,x}\,\mathrm{d}x = \left[\frac{1}{2}F_r^2\right]_0^L = 0 \tag{A7}$$

Note that the integration results of Eqs. (A5) and (A6) would be different from what is shown for the special case when $F_r \neq F_s$ but $\alpha_r = \alpha_s$.

For the case where $\alpha_r \neq \alpha_s$ and r and s even or r and s odd, we have

$$\frac{1}{L}\int_0^L F_r F_s\,\mathrm{d}x = \frac{2}{\alpha_r^4 - \alpha_r^4}\big[\alpha_r^3(A_s + C_s)(B_r - D_r) - \alpha_s^3(B_s - D_s)(A_r + C_r) - \alpha_s\alpha_r^2(B_s + D_s)(A_r - C_r) + \alpha_r\alpha_s^2(B_r + D_r)(A_s - C_s)\big] \tag{A8}$$

$$L\int_0^L F_r F_{s,xx}\,\mathrm{d}x = \frac{2}{\alpha_s^4 - \alpha_r^4}\big[\alpha_r^3\alpha_s^2(A_s - C_s)(B_r - D_r) - \alpha_s^3\alpha_r^2(B_s - D_s)(A_r - C_r) - \alpha_s^5(B_s + D_s)(A_r + C_r) + \alpha_r\alpha_s^4(B_r + D_r)(A_s + C_s)\big] \tag{A9}$$

$$L\int_0^L F_{r,x} F_{s,x}\,\mathrm{d}x = -L\int_0^L F_r F_{s,xx}\,\mathrm{d}x - 2\alpha_s(A_r + C_r)(B_s + D_s) \tag{A10}$$

For the case where $F_r = F_s$ and $\alpha_r = \alpha_s$, the integrals in Eqs. (A8–A10) become

$$\frac{1}{L}\int_0^L F_r F_r\,\mathrm{d}x = \frac{L^3}{\alpha_r^4}\int_0^L F_{r,x} F_{r,xxx}\,\mathrm{d}x = \frac{1}{2}\big[2A_r^2 - B_r^2 + 1\big] + \frac{A_r}{\alpha_r}[B_r + 1] \tag{A11}$$

$$L\int_0^L F_r F_{r,xx}\,\mathrm{d}x = -L\int_0^L (F_{r,x})^2\,\mathrm{d}x = -\frac{1}{2}\alpha_r^2\big[B_r^2 + 1\big] - A_r\alpha_r[B_r - 1] \tag{A12}$$

Again note that the integration results of Eqs. (A6–A10) would be different from what is shown for the special case when $F_r \neq F_s$ but $\alpha_r = \alpha_s$.

The terms with numerical superscripts in the right-hand sides of Eqs. (34–38) are defined as

$$
\begin{aligned}
E^1_{im} &= a^2\left[X^x_i X_{m,xx}\right]^a_0, & H^1_{im} &= a^2\left[X^x_{i,x} X_{m,x}\right]^a_0 \\
H^2_{im} &= a^2\left[X^y_{i,x} X_{m,x}\right]^a_0, & G^1_{im} &= a\left[X^x_i X_{m,x}\right]^a_0 \\
G^2_{im} &= a\left[X^x_i X_{m,x}\right]^a_0, & G^3_{im} &= a\left[X^x_i X^y_{m,x}\right]^a_0 \\
L^1_{im} &= \left[X^x_i X^x_m\right]^a_0, & L^2_{im} &= \left[X^y_i X^y_m\right]^a_0
\end{aligned}
\tag{A13}
$$

where in the case i odd, m even or i even, m odd, we have

$$
\begin{aligned}
E^1_{im} &= -2\left(A^x_i + C^x_i\right)\alpha^2_m (A_m - C_m) \\
H^1_{im} &= -2\alpha^x_i \alpha_m \left(B^x_i + D^x_i\right)(B_m + D_m) \\
H^2_{im} &= -2\alpha^y_i \alpha_m \left(B^y_i + D^y_i\right)(B_m + D_m) \\
L^1_{im} &= -2\left(A^x_i + C^x_i\right)\left(A^x_m + C^x_m\right) \\
L^2_{im} &= -2\left(A^y_i + C^y_i\right)\left(A^y_m + C^y_m\right)
\end{aligned}
\tag{A14}
$$

and in the case where i and m are both odd or even, we have

$$
\begin{aligned}
G^1_{im} &= -2\left(A^x_i + C^x_i\right)\alpha_m (B_m + D_m) \\
G^2_{im} &= -2\left(A^x_i + C^x_i\right)\alpha^x_m \left(B^x_m + D^x_m\right) \\
G^3_{im} &= -2\left(A^x_i + C^x_i\right)\alpha^y_m \left(B^y_m + D^y_m\right)
\end{aligned}
\tag{A15}
$$

To define and calculate M^1_{jn}, M^2_{jn}, F^1_{jn}, K^1_{jn}, K^2_{jn}, K^3_{jn}, J^1_{jn}, J^2_{jn}, and J^3_{jn}, we just need to change a by b, i by j, m by n, and X by Y and to use the appropriate coefficients from Y functions.

Acknowledgments

This research was supported partially by the NASA Langley Research Center under Grant NAG 1-1571 and by Mississippi State University. We would like to acknowledge the contributions of former graduate students Robert Harris and Timothy Clements in the early development and testing of the computer code used in this study.

References

[1]Carmichael, T. E., "The Vibration of a Rectangular Plate with Edges Elastically Restrained Against Rotation," *Quarterly Journal of Mechanics and Applied Mathematics*, Vol. 12, No. 1, 1959, pp. 29–42.

[2]Laura, P. A. A., and Grossi, R. O., "Transverse Vibrations of Rectangular Anisotropic Plates with Edges Elastically Restrained Against Rotation," *Journal of Sound and Vibration*, Vol. 64, No. 2, 1979, pp. 257–267.

[3]Warburton, G. B., and Edney, S. L., "Vibrations of Rectangular Plates with Elastically Restrained Edges," *Journal of Sound and Vibration*, Vol. 95, No. 4, 1984, pp. 537–552.

[4]Jones, K. M., and Klang, E. C., "Buckling Analysis of Fully Anisotropic Plates Containing Cutouts and Elastically Restrained Edges," *Proceedings of the AIAA/ASME/ASCE/AHS/ASC 33rd Structures, Structural Dynamics, and Materials Conference* (Dallas, TX), Pt. 1, AIAA, Washington, DC, 1992, pp. 190–200.

[5]Yu, Y. Y., "Flexural Vibrations of Elastic Sandwich Plates," *Journal of the Aerospace Sciences*, Vol. 27, No. 4, 1960, pp. 272–282.

[6]Chang, C. C., Ebcioglu, I. K., and Haight, C. H., "General Stability Analysis of Orthotropic Sandwich Plates for Four Different Boundary Conditions, Extension of the March–Erickson Approach," *ZAMM*, Vol. 42, No. 9, 1962, pp. 373–389.

[7]Rao, K. M., and Kaeser, R., "Shear Buckling of Stiff Core Anisotropic Sandwich Plate," *Journal of Engineering Mechanics*, Vol. 110, No. 9, 1984, pp. 1435–1440.

[8]Rao, K. M., "Buckling Analysis of Anisotropic Sandwich Plates Faced with Fiber-Reinforced Plastics," *AIAA Journal*, Vol. 23, No. 8, 1985, pp. 1247–1253.

[9]Libove, C., and Batdorf, S. B., "A General Small-Deflection Theory for Flat Sandwich Plates," NACA TN-1526, June 1948.

[10]Watanabe, N., Miyachi, K., and Daimon, M., "Stiffness and Vibration Characteristic of Sandwich Plates with Anisotropic Composite Laminates Face Sheets," *Proceedings of the AIAA/ASME/ASCE/AHS/ASC 34th Structures, Structural Dynamics, and Materials Conference* (La Jolla, CA), Pt. 1, AIAA, Washington, DC, 1993, pp. 236–244.

[11]Li, N., and Mirza, S., "Buckling Analysis of Clamped Sandwich Plates by the Reciprocal Theorem Method," *Computers and Structures*, Vol. 51, No. 2, 1994, pp. 137–141.

[12]Moh, J. S., and Hwu, C., "Optimization for Buckling of Composite Sandwich Plates," *AIAA Journal*, Vol. 35, No. 5, 1997, pp. 863–868.

[13]Whitney, J. M., *Structural Analysis of Laminated Anisotropic Plate*, Technomic, Westport, CT, 1987, pp. 44, 45.

[14]Reddy, J. N., *Mechanics of Laminated Composite Plates Theory and Analysis*, CRC Press, Boca Raton, FL, 1997, pp. 332, 333.

[15]Ueng, C. E. S., "Natural Frequencies of Vibration of an All-Clamped Rectangular Sandwich Panel," *Journal of Applied Mechanics*, Vol. 33, No. 3, 1966, pp. 683, 684.

[16]Harris, R. H., "Analysis and Design Optimization of Simply-Supported Rectangular Composite Sandwich Plates Under Axial and Biaxial Loading," M.S. Thesis, Dept. of Aerospace Engineering, Mississippi State Univ., Mississippi State, MS, Dec. 1995.

G. A. Kardomateas
Associate Editor